Liquid Crystals
Publication details, including instructions for authors and subscription information:
http://www.informaworld.com/smpp/title~content=t713926090

Optical and thermal properties of unsymmetrical liquid crystalline compounds based on isoxazole

Hugo Gallardo[a]; Fernando R. Bryk[a]; André A. Vieira[a]; Tiago E. Frizon[a]; Gilmar Conte[a]; Bruno S. Souza[a]; Juliana Eccher[b]; Ivan H. Bechtold[b]
[a] Departamento de Química, Universidade Federal de Santa Catarina, Florianópolis, SC, Brazil [b] Departamentode Física, Universidade Federal de Santa Catarina, Florianópolis, SC, Brazil

To cite this Article Gallardo, Hugo , Bryk, Fernando R. , Vieira, André A. , Frizon, Tiago E. , Conte, Gilmar , Souza, Bruno S. , Eccher, Juliana and Bechtold, Ivan H.(2009) 'Optical and thermal properties of unsymmetrical liquid crystalline compounds based on isoxazole', Liquid Crystals, 36: 8, 839 — 845
To link to this Article: DOI: 10.1080/02678290903072035
URL: http://dx.doi.org/10.1080/02678290903072035

Liquid Crystals,
Vol. 36, No. 8, August 2009, 839–845

Taylor & Francis
Taylor & Francis Group

Optical and thermal properties of unsymmetrical liquid crystalline compounds based on isoxazole

Hugo Gallardo[a]*, Fernando R. Bryk[a], André A. Vieira[a], Tiago E. Frizon[a], Gilmar Conte[a], Bruno S. Souza[a], Juliana Eccher[b] and Ivan H. Bechtold[b]

[a]*Departamento de Química, Universidade Federal de Santa Catarina, Florianópolis, SC – 88040-900, Brazil;* [b]*Departamento de Física, Universidade Federal de Santa Catarina, Florianópolis, SC – 88040-900, Brazil*

(Received 26 April 2009; final form 27 May 2009)

The thermal and optical properties of two series of unsymmetrical liquid crystalline compounds based on an isoxazole ring are described. Of these materials, **3–7** and **8–12** displayed strong absorption at 285 nm and a weak blue fluorescence in solution at around 377 nm, even with the presence of a high conjugated core. The fluorescence quantum yields observed varied from low to moderate (Φ_F = 1–62%), with large Stokes shifts (60–178 nm). All compounds exhibited liquid crystalline behaviour with a wide mesomorphism temperature range and characteristic phases of calamitic compounds, among them smectic A (SmA), smectic C (SmC) and nematic (N) phases. Their phases were characterised using polarising optical microscopy and differential scanning calorimetry. In addition, with X-ray diffraction experiments, layer spacing of 33.3–40.0 Å were observed for the smectic phases.

Keywords: isoxazole; X-ray diffraction; liquid crystals; luminescent materials

1. Introduction

Liquid crystals are fascinating materials with intermediate properties between those of solids and liquids. It is well known that molecular shape has a dominant influence on the existence of the liquid crystalline state (*1–10*). The design of novel thermotropic liquid crystals as advanced functional materials involves the suitable selection of a core fragment, linking group and terminal functionality. Over many years, a large number of liquid crystalline compounds containing heterocyclic units have been synthesised (*11–17*). Modern synthesis techniques allow researchers to access tailor-made materials with predictable properties, particularly in the field of liquid crystalline materials (*18–21*). The incorporation of heterocyclic moieties as core units in thermotropic liquid crystals can result in large changes in their mesophases and physical properties, because they possess more polarisable heteroatoms, such as nitrogen, oxygen and sulfur atoms. Interest in highly π-conjugated liquid crystal molecules containing heterocycles (*22–31*) has increased enormously in the past decade due to the possibility of their use in organic light-emitting diodes (OLEDs) (*32–34*), where electron-deficient heteroaromatic rings can potentially offer good charge-transport properties, together with their inherent self-organisation ability and strong fluorescence. In this regard, the isoxazole ring is a good candidate for materials science. In the early 1990s there was a flurry of interest in the isoxazole-based mesogens as calamitic liquid crystals, but the great difficulty in obtaining just one regioisomer of isoxazoles inhibited this area of study (*35–37*). However, with the improvements in synthesis methodologies, isoxazole chemistry may take on an important role within the field of liquid crystalline materials science. Isoxazoles are strong candidates for technological applications, particularly as emitters for optical devices or charge transporters for OLEDs.

Given the depth to which other classes of liquid crystals have been explored, the structure–property relationships of isoxazole liquid crystals still remain relatively uncharted, in particular the photophysical properties. In this context, our interest has been focused on luminescent liquid crystals containing the heterocycle isoxazole. Recently, we published (*38*) the synthesis of one series of unsymmetric liquid crystal compounds based on isoxazole (**3–7**), through the regioselective, simple and versatile reaction 1,3-dipolar cycloaddition, using different substituted chloro oximes and phenyl acetylenes catalysed by copper (I), and a second series prepared by Sonogashira cross-coupling (**8–12**).

Besides increasing the π-conjugation, the carbon–carbon triple bond in a liquid crystal molecule can also proportionately lead to a large birefringence (*39*, *40*). The aromatic groups (phenyl, naphthyl or phenylcarboxylate) were chosen to extend the rod-shaped liquid crystal molecules, which changes their length to width ratio, and also the extended π-conjugated system, with strong electron donating and withdrawing substituents. As a continuation of our work on π-extended heterocycle-based mesogens, we report in this paper the entire set of thermal and optical properties and X-ray diffraction (XRD) characteristics exhibited by

*Corresponding author. Email: hugo@qmc.ufsc.br

ISSN 0267-8292 print/ISSN 1366-5855 online

DOI: 10.1080/02678290903072035
http://www.informaworld.com

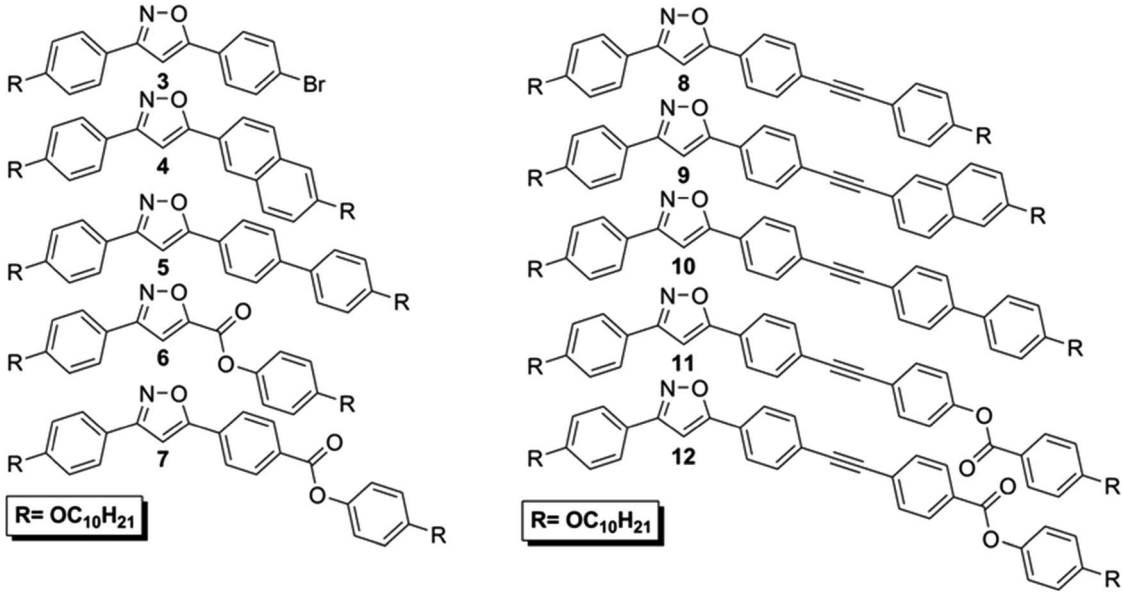

Figure 1. Chemical structures of compounds **3–12**.

these new unsymmetrical 3,5-disubstituted isoxazole liquid crystals (Figure 1).

2. Results and discussion

2.1 Thermal behaviour

The materials studied are divided into two series, **3–7** with an isoxazole ring and different chromophores and **8–12** with a triple bond increasing the rigid core and different aromatic moieties. These structures are shown in Figure 1. The thermal properties transition temperature, phase assignment and enthalpy energy of the compounds were investigated by thermal polarising optical microscopy (POM), differential scanning calorimeter (DSC) and thermogravimetric analysis (TGA). The results are summarised in Table 1. The optical observations were performed using clean untreated glass slides. All of the compounds exhibited liquid crystalline behaviour with characteristic phases of calamitic molecules.

The bar graph showing the mesophase range of these series can be seen in Figure 2. In order to understand the effects of varying the π-extended aromatic portion on the anisometry and mesomorphic behaviour of the materials, different aromatic systems linked to the isoxazole ring were investigated.

The bromide **3**, an intermediary used in the synthesis of molecules **8–12,** also showed mesomorphism behaviour, with smectic C (SmC) and smectic A (SmA) phases. The texture displayed by compound **3** was the typical fan shape of a SmA phase, with the formation of *bâtonnets* (*41*) from the cooling of the isotropic liquid at 179.4°C (Figure 3(b)).

Compounds **4**, **6** and **10** only presented the nematic (N) phase. Compound **6** exhibited the lowest melting point and lowest temperature range (ΔT = 40°C), while **10** showed the highest melting point and a very stable N phase (ΔT = 137°C). The isotropic fusion of **10** was not observed, just the beginning of the decomposition at 310°C. Figure 3 shows the DSC heating and cooling scans for compound **4**, and only a transition phase can be observed. The N phases were characterised by *schlieren* textures, and in Figure 4 curved dark brushes characteristic of N phases can be observed (Figure 4(a)).

In a more detailed study, compound **7**, containing phenylbenzoate, showed two smectic phases, SmC and SmA, rather than only SmA as stated in reference (*38*), and compound **12** displayed only the SmC phase. As can be seen by comparing **7** and **12**, the elongation by a phenyl and triple bond showed a wider mesomorphic range at around 36°C and the liquid crystalline phase presented by **7** was SmA and SmC, while that of **12** was only the SmC phase. The fan-shaped texture of compound **7** confirms that the SmA phase and the SmC phase were characterised by a *schlieren* texture (Figure 3(d)).

Compound **5** shows the SmA and N phases and compounds **8**, **9** and **11** also exhibited dimorphism with SmC and N phases; these compounds show a striking increase in mesophases with the length of the molecules. For compound **9**, thermal behaviour was observed, similar to other compounds with a triple connection with respect to the temperature range, the difference being the presence of SmA and N phases. With these results, one can make some observations: I)

Table 1. Phase transitions and enthalpies (kJ mol^{-1}) of compounds **3–12**[a].

3			Cr	99.6 (28.0) 75.0 (–29.2)	SmC	113.7 (9.38) 109.8 (–10.4)	SmA	184.6 (6.46) 179,4 (–6.9)	I	350°C
4					Cr	105.6 (57.87) 94.5 (–37.92)	N	186.0 (7.23) 183.0 (–7.36)	I	350°C
5			Cr	117.6 (45.37) 103.0 (–31.7)	SmA	135.9 (15.6) 132.4 (–14.2)	N	237.8 (10.37) 236.3 (–9.1)	I	373°C
6			Cr	73.6 (22.3)	Cr′	93.3 (35.8) 66.63 (–20.5)	N	133.9 (8.3) 127.3 (–10.6)	I	354°C
7	Cr	120.5 (24.1)	Cr′	130.0 (20.7) 112.7 (–28.7)	SmC	234.6 229.1[b]	SmA	244.2 (10.8) 238.0 (–2.1)	I	388°C
8	Cr	94.1 (16.2)	Cr(II)	125.5 (30.9) 107.6 (–17.3)	SmC	220.6 (2.9) 218.9[b]	N	240.1 (1.4) 237.4[b]	I	381°C
9	Cr	91.5 (7.0) 112.2 (–16.0)	Cr′	134.7 (34.9) 121.8 (–34.3)	SmC	234.0 (2.0) 228.9 (–6.7)	N	274.5 (2.6) 270.4 (1.9)	I	356°C
10			Cr	101.7 (47.7) 88.1 (–32.2)	Cr′	173.6 (8.0) 161.7 (–2.1)	N	> 310[b] ---	Dec.	310°C
11			Cr	130.4 (27.4) 109.8[b]	SmC	265.8 (33.5) 242.5[b]	N	316.5 (3.8)[b] 305.6[b]	Dec.	316°C
12			Cr	136.1 (27.1)	Cr′	139.2 (broad) 127.0 (–33.6)	SmC	300.2 (0.8) 289.5 (1.1)	I	390°C

Cr, Cr′ crystalline phases; SmA, smectic A phase; SmC, Smectic C phase; N, nematic phase; I, isotropic liquid; Dec., start decomposition.
[a]Determined by DSC for second heating and cooling cycle (scan rate 10°C min^{-1}).
[b]Determined by optical microscopy.
[c]Temperature of decomposition determind by TGA analysis, onset of decomposition in nitrogen, 10°C/min.

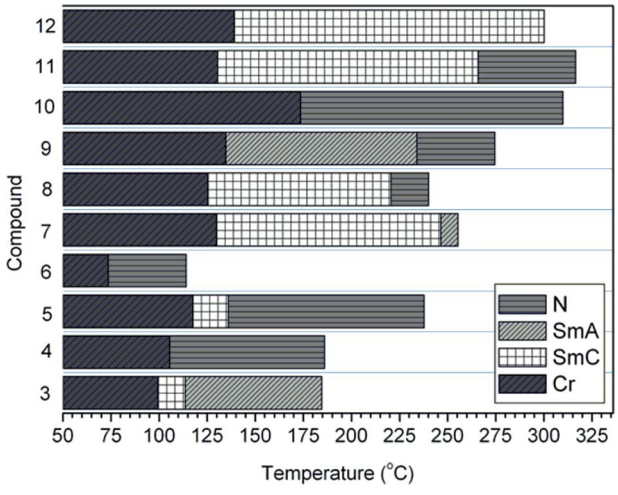

Figure 2. Bar graph showing a comparative mesomorphic profile of compounds **8–12**.

the smectogenic influence of the ester groups present in these isoxazole series, compounds **7**, **11** and **12**, show a clear tendency to develop smectic phases; II) for molecule **9**, the higher degree of anisometry in comparison to **4** favours the smectic mesomorphism; and III) in contrast to this trend the higher degree of anisometry in **5** compared to **10** confirms the disappearance of SmC. The decomposition temperatures of these materials are given in Table 1, starting at 310°C for compound **10** and increasing up to 390°C for **12.** These temperatures verified the high stability of the series.

2.2 X-ray diffraction studies

XRD experiments were carried out on compounds **7**, **9**, **11** and **12** to investigate the smectic structure exhibited by the mesophases. All the patterns recorded contain a sharp peak in the low-angle region, arising

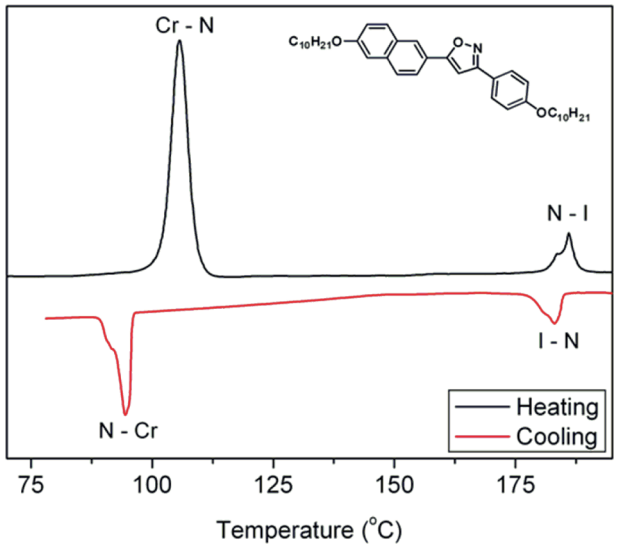

Figure 3. Second heating and cooling trace of **4**. This liquid crystalline compound showed only the N phase.

from the reflection of the X-ray beam on the smectic layers, and its corresponding higher order peak. The inter-layer spacing was obtained by applying Bragg's law to the first maximum. In addition, the molecular length of each compound was estimated using *ab initio* calculations at the HF/6 – 31G(d) level and the stationary points were located on the gas phase potential surface energy by careful variation of the atomic coordinates. The inclusion of one diffuse wave function on heavy atoms did not significantly alter the geometries found at the lower basis set. Figure 5 shows the pattern of compound **9** in the middle of the SmC phase at 170°C, where the smectic order was confirmed by the ratio of the value obtained for the inter-layer spacing (corresponding to the first maximum and denoted by $d_1 = 34.2 \pm 1$ Å) with respect to the value obtained for the second order peak (denoted by $d_2 = 17.0 \pm 1$ Å). It is well known that this ratio must obey the relation 1:2:3:4 in smectic phases; in our case $d_1/d_2 = 2.01 \pm 0.02$.

The inset of Figure 5 shows in detail the diffuse halo in the high-angle region related to the short-range correlations between neighbouring molecules in each layer. It corresponds to an average distance of $d3 = 4.5$ Å, which is consistent with the liquid-like arrangement of the molecules within the smectic layers. The same behaviour was observed for the four compounds investigated, except for a small shift of the first maximum in the low-angle reflection due to the different layer

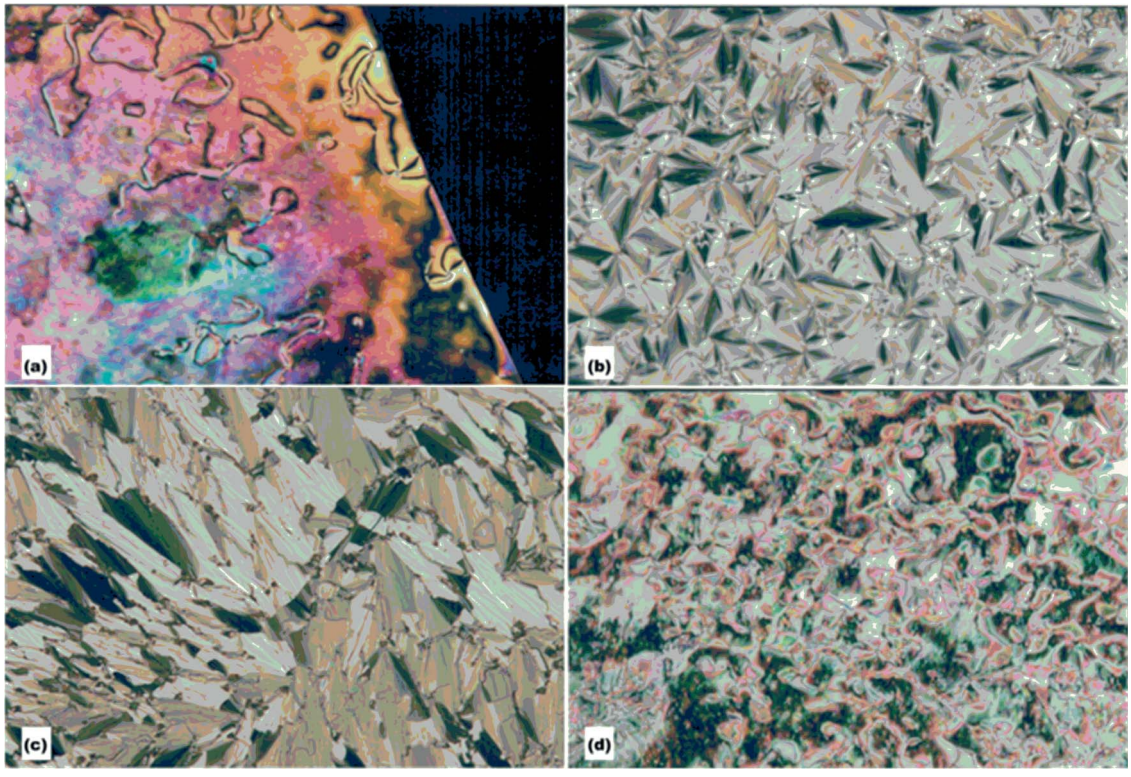

Figure 4. Photomicrographs of (a) the N phase *schlieren* texture at 235.5°C for compound **8**; (b) the SmA phase *focal-conic* texture at 120°C for compound **3;** (c) the SmC phase *broken fan-shaped* texture at 234°C for compound **9**; (d) the SmC phase *schlieren* texture at 120.7°C for compound **7**. Samples were sandwiched between untreated glass slides and viewed through crossed polarisers (33×).

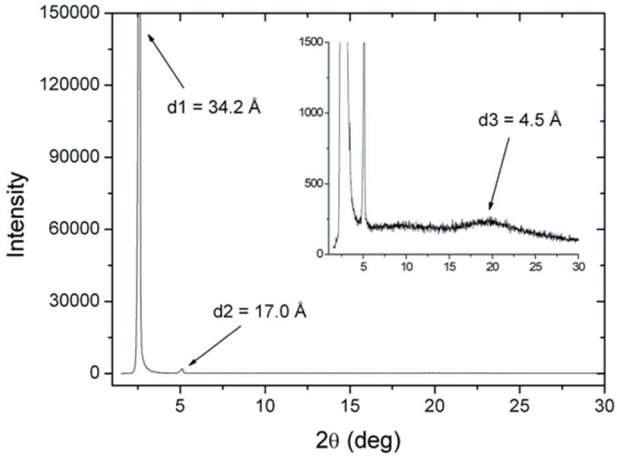

Figure 5. XRD pattern of compound **9**. Inset detail of the broad halo in the high-angle region.

spacing of the SmA and SmC phases. It is important to note that the SmA and SmC phases are known to present practically identical X-ray patterns, but they can easily be distinguished by the optical texture, as shown in Figure 4, and by the different layer spacing.

The measured and calculated values for the inter-layer spacing (d_m and d_c, respectively) are presented in Table 2.

For compound **7** in the SmA phase, where the molecules are positioned orthogonally to the smectic layers, despite the fact that the two values should be equivalent, the calculated value is 5.6 Å higher than that obtained from the X-ray experiments. However, the distance d_c obtained from the calculations considers the most-extended molecular conformation, i.e. with all their hydrocarbon chains in the *trans* arrangement, which is not necessarily the case in practice due to the conformational disorder of the aliphatic chains. In the SmC phase, the molecules adopt a tilted configuration with respect to the smectic planes; thus, a reduction in the inter-layer spacing is to be expected, as can be seen for compound **7** at 150°C.

Table 2. Results of the XRD for compounds **7**, **9**, **11** and **12**. Parameter d_c is the molecule length estimated using *ab initio* calculation at HF/6 – 31 G(d), d_m represents the layer spacing in the SmC and SmA phases and θ_m is the measured tilt angle

Compound	Temp (°C)/Phase	d_c (Å)	d_m (Å)	θ_m (degree)
7	233/SmA	43.7	38.1	–
	150/SmC		36.0	19
9	170/SmC	46.8	34.2	34
11	180/SmC	51.2	33.3	43
12	200/SmC	51.0	41.0	25

The tilt angle can be calculated using the simple relation $\theta = \cos^{-1}[d_m(\text{SmC})/d_m(\text{SmA})]$, which gives $\theta = 19$ degrees. Here, we considered that in the SmC phase the molecules maintain the length measured in the SmA phase and also do not adopt a more extended configuration. Regarding the tilt angles in the SmC phases of the other three compounds, which do not present SmA phases, we assumed that as in compound **7**, the molecule length in the mesophase is reduced by a factor of around 5.6 Å compared to the fully-extended length obtained from the calculations. This seems reasonable, given that the other three compounds contain the same hydrocarbon chains, since the contribution of the different mesogenic cores to the conformational freedom is not significant. The tilt angles obtained are also shown in Table 2. By comparing the values of compounds **7**, **9** and **12**, the inter-layer spacing slightly decreases as the molecular length increases, accompanied by an increase in the tilt angle. An exception is observed for compound **11**, where there is a significant decrease in the inter-layer spacing in the SmC phase compared to compound **12**, which has approximately the same extended molecular length. This phenomenon can be explained by the inversion of the ester group in molecules **11** and **12**. When the carbonyl group is linked directly to the rigid core, the anisometry of the system remains linear, as can be observed in **12**, but when the carbonyl is replaced by the oxygen in **11,** the anisometry seems to be 'broken' and the length of the layers is shorter. These differences were also observed in the respective phases.

2.3 Absorption and fluorescent properties

The ultraviolet (UV)-vis absorption and fluorescence spectroscopic data of isoxazole-based compounds **3–12** in chloroform are summarised in Table 3.

All synthesised compounds displayed similar absorption and fluorescence spectra. These compounds showed a maximum absorption peak at around 307 nm and an intense absorption band peaking between 245 and 311 nm (Figure 6). These absorption bands are assigned to the π–π* transition due to their high molar absorption coefficients ($\varepsilon = 2.3 \times 10^{-5} - 4.6 \times 10^{-6}$ mol^{-1} cm^{-1}). Compound **3** displayed two pronounced bands at 256 and 284 nm, but this effect was not observed for the other compounds, while **5**, **9** and **12** showed broad bands. Compounds **5**, **6** and **7** exhibited a hypsochromic shift of around 60 nm in comparison to the other materials.

Compounds **3–12** showed a weak blue emission in solution under a UV-vis lamp (λ_{em}^{max} 347–423 nm) with large Stokes shifts (60–178 nm). The quantum yields of luminescence for these materials were determined

Table 3. Summary of photophysical properties of compounds **3–12**, in $CHCl_3$ solution

Compound	λ_{abs}^{max}/nm (ε)[a]	λ_{em}^{max} /nm	Stokes shift/nm	Φ_{PL}[b]
3	255; 289 (1.6. 10^6)	349	60	0.02
4	303 (2.4. 10^5)	369	66	0.32
5	248 (1.6. 10^6)	380	132	0.18
6	246; 278 (2.3. 10^5)	424	178	0.01
7	286 (1.0. 10^6)	380	94	0.27
8	309 (7.6. 10^5)	418	109	0.05
9	288; 311; 345[c] (1.2. 10^6)	380	69	0.51
10	310 (4.6. 10^6)	396	86	0.61
11	303 (4.4. 10^6)	366	63	0.03
12	315; 334 (1.5. 10^6)	377	62	0.02

[a]Units = $mol^{-1}cm^{-1}$. [b]Determined using PBD as the standard (Φ_{PL} = 0.546). [c]Shoulder peak.

using the standard 2-phenyl-5-(4-diphenylyl)-1,3,4-oxadiazole (PBD). In general, these compounds give low fluorescence quantum yields (Φ_F), as noted for **3**, **6**, **8**, **11** and **12**, which produced very low quantum yields of around 1–5%. Molecules **4**, **7** and **10** gave modest photoluminescence quantum yields (27–61%).

3. Conclusions

A study of the thermal and photophysical properties was performed on two series of compounds derived from the isoxazole ring. All of the compounds **3–7** and **8–12** displayed liquid crystalline behaviour. These compounds displayed wide temperature ranges of mesomorphism, notably compounds **10**, **11** and **12**, with more than 130°C of mesomorphism. In general, compounds **3–7** showed lower liquid crystalline profiles than molecules **8–12** with an expansive core, resulting from anisometry. The phases observed using POM were SmA, SmC and N, with schlieren textures and fan-shaped structures. The XRD confirmed the respective smectic phases observed, with layer spacing of 33.3–40.0 Å. Materials **3–12** displayed strong absorption at around 285 nm and emission at 377 nm in a chloroform solution. The fluorescence quantum yields observed varied from low to moderate (Φ_F = 1–62%) and showed large Stoke shifts (60–178 nm).

4. Experimental

4.1 Materials

The synthesis of compounds **3–7** was carried out through the 1,3-dipolar cycloaddition reaction, using different substituted chloro oximes and phenyl acetylenes, and materials **8–12** were prepared through the Sonogashira reaction from 5-(4-bromophenyl)-3-(4-(decyloxy)phenyl)isoxazole and different aryl acetylenes (*42*).

4.2 Equipment

The melting points, thermal transitions and mesomorphic textures were determined using an Olympus BX50 microscope equipped with a Mettler Toledo FP-82 hot stage and a PM-30 exposure control unit. An HP UV-vis model 8453 spectrophotometer was used to record absorption spectra. Fluorescence spectra were recorded on a Hitachi-F-4500 fluorescence spectrophotometer. The X-Ray diffraction experiments were carried out with XPERT-PRO (PANalytical) diffractometer system using the linear monochromatic Cu Kα_1 beam (λ = 1.5405 Å), with applied power of 1.2 kVA. The scans were performed in continuous mode from 2° to 30° and the diffracted radiation

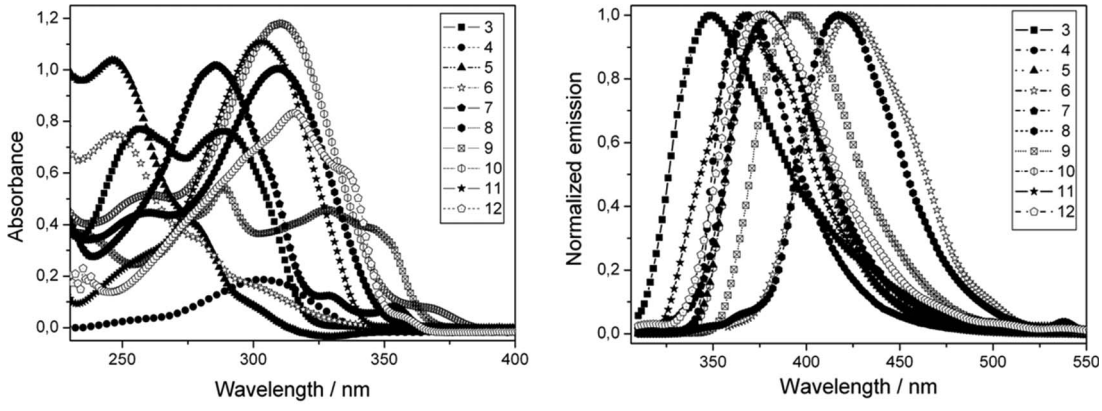

(a) (b)

Figure 6. (a) Absorption and (b) fluorescence spectra of compounds **3–12** in chloroform.

collected with an X'Celerator detector. The samples were prepared by prior heating (with a hot stage) of an amount of powder on a glass plate until the mesophase temperature was reached, followed by a cooling process until solidification took place. As a result, we obtain a film of around 1 mm thickness. The film was then placed in the diffractometer chamber on the TCU2000 – Temperature Control Unit (Anton Paar), which allows precise control of the sample temperature during measurement. The films were first heated until the isotropic or N phase and the diffraction patterns were collected during cooling

Acknowledgements

The authors thank Conselho Nacional de Desenvolvimento Científico e Tecnológico (CNPq – Brazil), INCT-cat, FAPESC, IMMP-MCT and the Laboratório de Difração de Raios-X (LDRX-CFM/UFSC) for the X-ray diffraction experiments.

References

(1) Demus, D.; Goodby, J.; Gray, G.W.; Spiess, H.-W.; Vill, V., Eds. *Handbook of Liquid Crystals*; VCHWiley: Weinheim, 1998; ch 1.
(2) Goodby, J.W.; Bruce, D.W.; Hird, M.; Imrie, C.; Neal, M.J. *Mater. Chem.* **2001**, *11*, 2631–2636.
(3) Cristiano, R.; Gallardo, H.; Bortoluzzi, A.J.; Bechtold, I.H.; Campos, C.E.M.; Longo, R.L. *Chem. Commun.* **2008**, 5134–5136.
(4) Cai, R.; Samulski, E.T. *Liq. Cryst*. **1991**, *9*, 617–634.
(5) Cristiano, R.; Westphal, E.; Bechtold, I.H.; Bortoluzzi, A.J.; Gallardo, H. *Tetrahedron* **2007**, *63*, 2851–2858.
(6) Gallardo, H.; Favarin, I. *Liq. Cryst.* **1993**, *13*, 115–125.
(7) Vasconcelos, U.B.; Schrader, A.; Vilela, G.D.; Borges, A.C.A.; Merlo, A.A. *Tetrahedron* **2008**, *64*, 4619–4626.
(8) Parra, M.L.; Saavedra, C.G.; Hidalgo, P.I.; Elgueta, E.Y. *Liq. Cryst*. **2008**, *35*, 55–64.
(9) Gallardo, H.; Maurmann, L. *Mol. Cryst. Liq. Cryst.* **2002**, *378*, 23–34.
(10) Merlo, A.A.; Braun, J.E.; Vasconcelos, U.; Ely, F.; Gallardo, H. *Liq. Cryst*. **2000**, *27*, 657–663.
(11) Bartulín, J.; Martinez, R.; Gallardo, H.; Muller, H.; Taylor, T.R. *Mol. Cryst. Liq. Cryst*. **1993**, *225*, 175–182.
(12) Cristiano, R.; Vieira, A.A.; Ely, F.; Gallardo, H. *Liq. Cryst*. **2006**, *33*, 381–390.
(13) Aldred, M.P.; Vlachos, P.; Dong, D.; Kitney, S.P.; Tsoi, W.C.; O'Neill, M.; Kelly, S.M. *Liq. Cryst*. **2005**, *32*, 951–965.
(14) Paraskos, A.J.; Swager, T.M. *Chem. Mater.* **2002**, *14*, 4543–4549.
(15) Kauhanka, M.U.; Kauhanka, M.M. *Liq. Cryst*. **2006**, *33*, 121–127.
(16) Cristiano, R.; Santos, D.M.P.O.; Gallardo, H. *Liq. Cryst*. **2005**, *32*, 7–14; Cristiano, R.; Ely, F.; Gallardo, H. *Liq. Cryst*. **2005,** *32*, 15–25.
(17) Meyer, E.; Zucco, C.; Gallardo, H. *J. Mater. Chem.* **1998**, *8*, 1351–1354.
(18) Tavares, A.; Schneider, P.H.; Merlo, A.A. *Eur. J. Org. Chem.* **2009**, *6,* 889–897.
(19) Passo, J.A.; Videla, G.D.; Schneider, P.H.; Ritter, O.M.S.; Merlo, A.A. *Liq. Cryst.* **2008**, *35*, 833–840.
(20) Gallardo, H.; Ely, F.; Bortoluzzi, A.J.; Conte, G. *Liq. Cryst*. **2005**, *32*, 667–671.
(21) Conte, G.; Ely, F.; Gallardo, H. *Liq. Cryst*. **2005**, *32*, 1213–1222.
(22) Vieira, A.A.; Cristiano, R.; Bortoluzzi, A.J.; Gallardo, H. *J. Mol. Struct*. **2008**, *875*, 364–371.
(23) Conte, G.; Cristiano, R.; Ely, F.; Gallardo, H. *Synth. Commun.* **2006**, *36*, 951–958.
(24) Tokuhisa, H.; Era, M.; Tsutsui, T. *Appl. Phys. Lett*. **1998**, *72*, 2639–2641.
(25) Inomata, H,; Gouchi, K.; Masuto, T.; Konno, T.; Imai, T.; Sasabe, H.; Brown, J.J; Adachi, C. *Chem. Mater*. **2004**, *16,* 1285–1291.
(26) Attias, A.-J.; Cavalli, C.; Donnio B.; Guillon, D.; Hapiot, P.; Malthête, *J. Chem. Mater.* **2002**, *14*, 375–384.
(27) Marcelo, N.F.; Vieira, A.A.; Cristiano, R.; Gallardo, H.; Bechtold, I.H. *Synth. Met.* **2009**, *159*, 675–680.
(28) Vlachos, P.; Mansoor, B.; Aldred, M.P.; O'Neill, M.; Kelly, S.M. *Chem. Commun*. **2005**, 2921–2931.
(29) Qu, S.; Li, M. *Tetrahedron* **2007**, *63*, 12429–12436.
(30) Majumdar, K.C.; Pal, N.; Debnath, P.; Rao, N.V.S. *Tetrahedron Lett.* **2007**, *48*, 6330–6333.
(31) Sonntag, M.; Strohriegl, P. *Tetrahedron Lett.* **2006**, *47*, 8313–8317.
(32) O'Neill, M.; Kelly, S.M. *Adv. Mater*. **2003**, *15*, 1135–1146.
(33) Hohnholz, D.; Steinbrecher, S.; Hanack, M. *J. Mol. Struct*. **2000**, *521*, 231–237.
(34) Zhang, X.-B.; Tang, B.-C.; Zhang, P.; Li, M.; Tian, W.-J. *J. Mol. Struct*. **2007**, *846*, 55–64.
(35) Brown, D.H.; Styring, P. *Liq. Cryst.* **2003**, *30*, 23–30.
(36) Barbera, J.; Cativiela, C.; Serrano, J.L.; Zurbano, M.Z. *Liq. Cryst.* **1992**, *11*, 887–897.
(37) Katritzky, A.R.; Wang, M.; Zhang, S.; Voronkov, M.V. *J. Org. Chem.* **2001**, *66,* 6787–6791.
(38) Vieira, A.A.; Bryk, F.R.; Conte, G.; Bortoluzzi, A.J.; Gallardo, H. *Tetrahedron Lett.* **2009**, *50*, 905–908.
(39) Wu, S.-T.; Finkenzeller, U.; Rieffenrath, V. *J. Appl. Phys*. **1989**, *65*, 4372–4376.
(40) Xianyu, H.; Gauza, S.; Song, Q.; Wu, S.-T. *Liq. Cryst*. **2007**, *34*, 1473–1478.
(41) Dierking, I. *Textures of Liquid Crystal*; Wiley-VCH: Weinheim, 2003.
(42) Gallardo, H.; Cristiano, R.; Vieira, A.A.; Neves Filho, R.A.W.; Srivastava, R.M. *Synthesis* **2008**, *4*, 605–609; Gallardo, H.; Cristiano, R.; Vieira, A.A.; Filho, R.A.W.N.; Srivastava, R.M.; Bechtold, I.H. *Liq. Cryst*. **2008,** *35,* 857–863.